Journal of Cleaner Production 175 (2018) 624–640

Contents lists available at ScienceDirect

Journal of Cleaner Production

journal homepage: www.elsevier.com/locate/jclepro

Influence of technical failures on the performance of an optimized community-size solar heating system in Nordic conditions

Hassam ur Rehman*, Janne Hirvonen, Kai Sirén

Aalto University, School of Engineering, Department of Mechanical Engineering, HVAC Group, PO Box PL 14400/Vi 351, 00760 Aalto, Finland

ARTICLE INFO

Article history:
Available online 22 December 2017

Keywords:
Solar Community
Seasonal storage
Solar district plant failures
Cold climate
District heating
Multi-objective optimization

ABSTRACT

There is a substantial need to accelerate the advancement and implementation of clean energy technologies in order to solve the challenges of the energy crisis and climate change. Solar heating technology is a feasible solution among clean energy technologies. In real conditions such complex systems often suffer from different kinds of technical failures and deviations reducing the system performance. This paper focuses on the challenges of a solar district heating system at high latitudes, proposes an optimized solution and investigates the influence of possible failures in planning, implementation and operation phase. The configuration proposed is a heat pump connected between two tanks, using solar-charged borehole storage to directly charge the lower temperature tank. Dynamic simulations were performed and a multi-objective optimization was carried out. The impact of the considered system solutions on the renewable energy fraction, purchased electricity and investment cost as a function of demand, solar thermal and photovoltaic areas, tanks and borehole volumes have been evaluated. The influence of 10 different technical failures was investigated. The study showed that in the optimized system, the most serious faults were i) de-stratification of the storage tanks (23–35% increase in annual purchased electricity) ii) on-off instead of variable speed control of the solar circulation pump (1–22% increase) and iii) reduction in heat pump performance (7–21%). These numbers of course depend on the initial assumptions, but still they show the magnitude of performance reduction some failures can achieve. Therefore, these parameters need to be considered during the implementation of such a system.
© 2017 Elsevier Ltd. All rights reserved.

1. Introduction

Huge environmental problems are an increasing worldwide issue due to fossil fuel consumption. Efforts are being made to develop and introduce energy-efficient and environmentally friendly systems through the utilization of renewable energy (The European Parliament and the Council of the European Union, 2010). Buildings are one of the largest energy consumers and emitters of CO_2, representing 40% of the European Union's total energy consumption (The European Parliament and the Council of the European Union, 2010). Moreover, in Finland more than 80% of residential energy consumption is used for space heating and domestic hot water heating, which increased by 5% since 2015 (Official Statistics of Finland (OSF), 2016), causing CO_2 emissions to increase by 8% each year (Official Statistics of Finland (OSF), 2016). Therefore, there is now renewed interest in the use of renewable energy due to the environmental impact (Bose, 2016). In Finland, most of the population lives in areas receiving more than 1472.2 kWh/m^2 total solar radiation annually. Hence, there is substantial potential for harvesting solar energy (Riku Pasonen, 2012; Jylhä et al., 2015).

Solar district heating with seasonal storage is a very promising alternative to fossil fuel heating and are researched by several entities, such as the IEA's Task 32 (International Energy Agency Solar Heating and Cooling Programme, IEA-SHC, Task 32, 2015). Solar thermal (ST) systems are key technologies for achieving emission reduction goals, and their use is spreading in European countries (European solar thermal industry federation(ESTIF), 2017; Dalenbäck and Werner, 2012; Schmidt et al., 2004; Nielsen, 2012). Numerous solar district heating and seasonal sensible thermal storage projects have seen the light of day in Europe and North America. There are large-scale pilot plants located in Germany, Sweden, Denmark, and Canada (Mangold, 2007; Lundh and Dalenbäck, 2008) that use solar energy integrated with seasonal storage (McDowell and Thornton, 2008; Sibbitt et al., 2012).

* Corresponding author.
E-mail address: hassam.rehman@aalto.fi (H. Rehman).

https://doi.org/10.1016/j.jclepro.2017.12.088
0959-6526/© 2017 Elsevier Ltd. All rights reserved.

Nomenclature

BTES	Boreholes thermal energy system
C_B	Building investment cost (€/m_2)
C_{BTES}	Boreholes cost (€/m_3)
C_{Fins}	Building floor insulation cost (€/m_3)
C_{HR}	Building heat recovery cost (€)
C_{HT}	Hot tank cost (€/m_3)
C_{PV}	Photovoltaic panels cost (€/m_2)
C_{Rins}	Building roof insulation cost (€/m_3)
C_{ST}	Solar thermal collectors cost (€/m_2)
C_{WIND}	Building windows cost (€/m_2)
C_{Wins}	Building walls insulation cost (€/m_3)
C_{WT}	Warm tank cost (€/m_3)
CO_2	Carbon dioxide
COP	Coefficient of performance
DHW	Domestic hot water
DLSC	Drake Landing Solar Community
E_{BH}	Direct electric backup heater electricity consumption (kWh/m_2/yr)
E_{BUL}	Building appliances electricity consumption (kWh/m_2/yr)
E_{EXP}	Exported electricity to the grid (kWh/m_2/yr)
E_{HP}	Heat pump electricity consumption (kWh/m_2/yr)
E_{PUMP}	Auxiliary pumps electricity consumption (kWh/m_2/yr)
E_{PUR}	Purchased electricity from the grid (kWh/m_2/yr)
ESTIF	European solar thermal industry federation
EU	European Union
F1	First objective function (purchased electricity)
F2	Second objective function (investment costs)
HP	Heat pump
HVAC	Heating, ventilation, and air conditioning
IC	Investment costs
IEA	International energy agency
MOBO	Multi-objective building optimizer
NSGA-II	Non-dominated Sorting Genetic Algorithm II
OSF	Official statistics of Finland
PV	Photo voltaic panels
SH	Space heating
SHC	Solar heating cooling
ST	Solar thermal collectors
TES	Thermal energy storage

With few exceptions, the performance of the plants has been quite acceptable when they are considered as field trials of new designs (Internatonal Energy Agency-Task VII, 1990). Although performance lives up to expectations in some installations, this is not always the case. In some cases, the solar collector performances are overestimated and the heat store losses are underestimated. There are several reasons for this. One reason is that no proper tools for pre-design studies were used. Other reasons are that incorrect inputs are used, the design tools are applied in the wrong way or not validated, and optimization issues (Neves and Silva, 2014) related to size and cost. It is not surprising that performance has not always met expectations, since theoretical models used in pre-studies describe performance under ideal conditions. Many operation problems are related to an incorrect use of various technologies. Several publications have previously discussed several solar heating plants with seasonal storage with regards to system design and costs (Schmidt et al., 2004; Meliß and Späte, 2000; Fisch et al., 1998). Several authors have discussed simulation related to solar heating plants with and without seasonal storage along with several types of backup systems (Raab et al., 2005). Publications based on monitoring data are rare, and the ones available are often restricted to laboratory scale or one single system (Hahne, 2000). However, there has been little research carried out to analyze the performance of the real system using monitored data and comparing it with estimated or predicted results (Bauer et al., 2010). It is interesting to find that the measured and estimated values have discrepancies, caused for several reasons. These causes are crucial when designing solar thermal district plants, as they can affect the performance and solar fraction of the plant and might need to be considered during the estimation phase.

In Europe, about 1.1 million m^2 of solar collectors has been installed by 2001, corresponding to about 5500 MW of thermal power (Schmidt et al., 2004; Bauer et al., 2010). Out of this, 60 MW of thermal power is installed in large systems with collector areas of 500 m^2 or more. Some of these largest ten plants are situated in Germany, Sweden, and Denmark. There are 28 systems with collector areas between 1000 and 2700 m^2 and 27 systems with collector areas between 500 and 1000 m^2. Four different types of seasonal thermal energy stores are developed, tested, and monitored under realistic operation conditions (Bauer et al., 2010). Hot-water thermal energy store (Friedrichshafen), gravel-water thermal energy store (Steinfurt-Borghorst), borehole thermal energy store (Neckarsulm), and aquifer thermal energy store (Rostock). In Friedrichshafen, results showed that the measured solar fraction varied from 21 to 33%. However, it is estimated that the solar fraction could reach 43%. This value has not yet been reached because of a higher than expected demand, higher thermal losses due to insulation and higher net temperatures in space heating circuits, a reduction in collectors, and heat exchanger efficiency (Bauer et al., 2010). Similarly, in Neckarsulm (Bauer et al., 2010; Urbaneck et al., 2015), Rockstock (Bauer et al., 2010; Urbaneck et al., 2015), and Eggenstein (Bauer et al., 2010; Urbaneck et al., 2015), the measured and estimated performance showed discrepancies. The design solar fractions are overestimated, and measurements showed that in a real application, the systems underperformed. The main common reasons found are, a higher than expected net return temperature, efficiency issues in the heat exchanger and collector, losses through storage, and wrong sizing due to non-optimized solutions (Bauer et al., 2010; Urbaneck et al., 2015). In the project installed and monitored in Steinfurt-Borghorst, Hamburg, and Neckarsulm II, the results showed a deviation between the designed performance and the monitored performance. The main issues reported are the heat exchanger performance issue, heat losses in the seasonal storage and tanks, higher net return temperature, and a smaller solar thermal collector area than planned (BINE Information Service, 2000). In Crailsheim-Hirtenwiesen (Federal Ministry for the Environment, Nature Conservation and Nuclear Safety (BMU, 2013), a solar thermal energy system is intended to cover 50% of the heating requirements of a residential area. To ensure this possibility throughout the year, seasonal storage has been installed with a volume of 10,000 m^3 of water equivalent. It is found that system performance is less than expected due to losses through the ground and the higher operating temperature of the space heating network. Leakages reported in Crailsheim, Germany (Nussbicker-Lux, 2012) reduced the performance of the solar district heating. Another report related to the Drake Landing Solar Community in

Canada (Sibbitt et al., 2015) discusses the practical issues and uncertainty faced by the solar thermal system. The reasons behind the underperformance of the system compared to the simulated results are thermal properties of the borehole storage, tank stratification issues, pump controls, heat losses through the network due to high temperatures, and lower than expected collector efficiency. Hence, it shows that these common reasons are the main causes that can affect the performance of the system and cause a deviation in the measured and estimated performance (Bauer et al., 2010; Urbaneck et al., 2015). Other than the above-mentioned issues, some other reasons can also decrease the performance of the system. Claudia Weissmann et al. (Weissmann et al., 2017) and Liuhua Gao et al. (Gao et al., 2015) estimated that building orientation, demand, solar thermal collector orientation and size (Bauer et al., 2016), insulation losses, pipe leakages (Nussbicker-Lux, 2012), and seasonal storage losses can affect the system performance.

Moreover, in analyses of solar district heating networks elsewhere in the European Union, similar issues are mentioned. Fifteen years of research and development in central solar heating in Denmark is done by Alfred (Heller, 2000), who found that heat exchanger efficiency and component sizing issues are faced in most of the cases. Furthermore, researchers (Tordrup et al., 2017) found issues in the boreholes boundary layer conductivity. It changed from the predicted value that altered the performance of the district heating system implemented in Brædstrup, Denmark. Jan-Olof Dalenbäck (2005) discusses solar communities and a solar thermal district heating network in Sweden. Sweden has a leading role in the early demonstrations of such systems. It is found that the insulation of tanks and the space heating net temperature affect the performance of the system. Furthermore, ground properties, heat exchanger efficiency, and solar collector efficiency are important parameters based on the Swedish and German experiences (Ochs et al., 2008; Dalenbaeck, 1998).

In Finland, Eko-Viikki is a test site for ecological construction located in southern Latokartano, Helsinki. The apartments are constructed in 2000–2004. Reports are found (Hakaste et al., 2008; Faninger-Lund, 2003) (Faninger-Lund, 2003; SOLPROS, 2004) that mentioned that the average energy demand of the solar district heating demand exceeded expectations. Some of the major reasons behind the underperformance of the system are: firstly, higher demand of the building than designed for due to heat recovery efficiency issues, ventilation issues, and windows not performing as expected. Secondly, the solar thermal energy system is not performing as designed due to lower tanks sizes, smaller tilt angle of the collectors, under sizing of the collector area, higher net temperature of the space heating network, and overall optimization issues.

The aim and objective of this research is to estimate the influence of failures and defects in the technical parameters on the performance of the optimized solar energy system. The novelty and innovation in this paper is the detailed and systematic failure analysis of solar district heating system, for a community sized heating demand in Nordic region. The failure analysis is done based on real condition issues that can occur during the lifetime of the system operations as reported by previous research. The challenges (described above) of this location are addressed and solutions are proposed in this study based on the technical and economic aspects. Purchased electricity and investment costs (IC) are the two objectives that were minimized. In addition, the heating renewable energy fraction is also evaluated to analyze overall performance. The design variables considered for the optimization are solar thermal (ST) area, short-term storage tank volume, borehole volume, photovoltaic area, and building design. Furthermore, a detailed focus is made on the technical failures and defects such as heat exchanger efficiency, solar thermal collector intercept efficiency, tank stratification, annual average heat pump coefficient of performance (COP), space heating temperature differences, hot and warm tank charging set points, space heating supply temperature set points, solar thermal collectors pump circulation, and thermal conductivity of boreholes boundary to estimate the deviation in non-dominated optimized solutions caused by these factors. The study is performed using the dynamic simulations approach using TRNSYS (Solar Energy Laboratory, University of Wisconsin-Madison, 2012) due to the complexity of the proposed system (Rad et al., 2013; Montagud et al., 2013). MOBO (multi-objective building optimizer) (Palonen et al., 2013) is used to run the NSGA-II algorithm and TRNSYS model together for the optimization of two objectives.

2. Energy system

The study is performed on a virtual Finnish community with a dedicated solar district heating network. It is modeled on TRNSYS 17 and introduced earlier in (Rehman et al., 2017). The community consists of 100 houses with a heated area of 100 m^2each. The solar thermal collector is connected with two centralized short term storage tanks (high and low temperature) and borehole thermal energy storage (BTES) system. Heat pump (HP) is integrated to provide heating energy during the absence of solar energy. The on-site electricity is generated through photovoltaic panels (PV). The on-site demand of energy system (pumps, heat pumps and backup electric heaters) and building appliances are primarily met through locally generated solar electricity. Furthermore, electricity is imported or exported via grid to compensate the mismatch between electricity demand and generation. A schematic representation of the system is shown in Fig. 1. The green lines represent the electricity flows, while the rest of the solid lines show the heat flows in Fig. 1. The Hot, warm and cold temperature heat flows are represented by red, orange and blue colors solid lines in Fig. 1.

The solar collectors are connected to the short term storage tanks in parallel. When the tanks needed charging, the first option is to use the solar collector. If the warm tank temperature is lower than 40 °C, it is heated to 45 °C. And for the hot tank, if the temperature is lower than 65 °C, it is heated to 70 °C by the solar collectors in parallel (Rehman et al., 2016). If both tanks are at adequate temperature levels, all the solar heat is pumped into the warm tank to maximize energy efficiency. If no energy is available from the solar collectors, heat could be directly transferred from BTES into the warm tank in order to charge the tank. Cold fluid entered from the cool outer edge of the BTES and exited from the hot center. If the warm tank temperature is less than 35 °C and the BTES's average temperature is higher than the warm tank's top temperature, the energy is transferred via the BTES. The energy from the warm tank is used by the heat pump (HP) to heat the hot tank in need of energy when ST energy is not available. If the hot tank temperature is lower than 60 °C, it is heated to 65 °C by the HP (Rehman et al., 2016). The warm tank is charged from the BTES every time the HP is used to charge the hot tank. Heat is transferred to BTES to avoid overheating the short-term tanks.

Heat from the warm storage tank is transferred when the tank temperature reached 50 °C, and the process stopped once the temperature dropped to 45 °C. Heat is transferred from the hot storage tank when the tank temperature reached 75 °C and stopped once the temperature goes below 70 °C (Rehman et al., 2017). The space heating (SH) is provided by passing the SH water through the warm tank and if necessary through the hot tank. This heated water is then provided to the houses at a temperature between 30 °C and 40 °C, depending on the outdoor temperature. Domestic hot water (DHW) is provided to houses by preheating the cold water in the warm tank and then heating the water further in the hot tank until

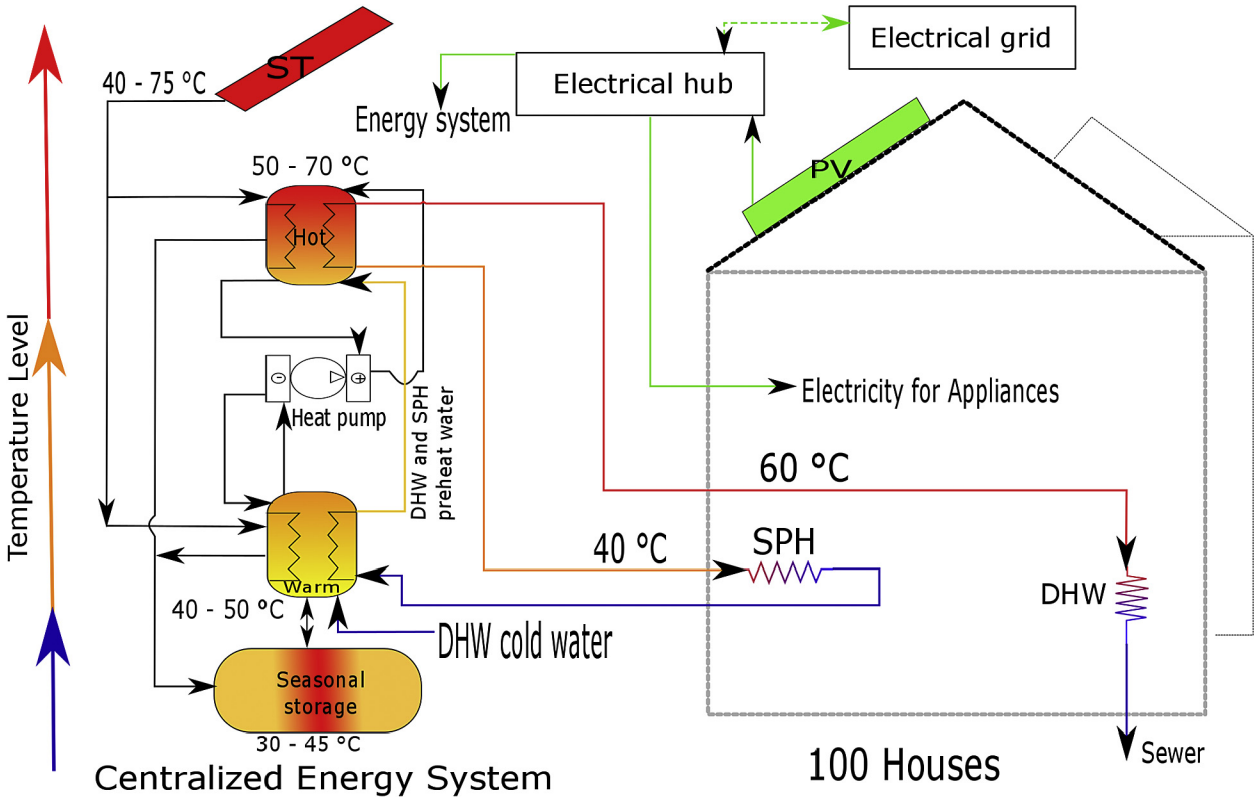

Fig. 1. Simple schematic representation of the energy system.

it reached the desired temperature of 60 °C. There is also a DHW recirculation circuit in the system to ensure that DHW is continuously available without delay. If the HP and solar energy are not enough to meet the temperature needs, backup heating is handled by direct electric heaters. Based on previous studies, the connection between the short-term storage tank and the ST collectors is chosen to be parallel (Rehman et al., 2017). Secondly, temperature tracking control mode is selected (Rehman et al., 2017) where the collector typically aims for an outlet temperature that is one degree higher than the tank's top temperature. The cooling needs in the community are minute, therefore the cooling system is not included.

3. Optimization methodology

3.1. Problem definition

The focus in this paper is on failure analysis and its effect on the optimized system. Therefore, firstly, the energy system is optimized using a multi-objective optimization algorithm (NSGA-II), where purchased electricity and investments are minimized together in ideal conditions. Lastly, the technical failures and system defects are included to analyze the effects of these defects on the performance of the optimized system under real (non-ideal) conditions. The renewable energy fraction (Rehman et al., 2017), final purchased electricity, and investment costs (IC) are calculated to evaluate the system.

In a solar district heating system, an optimization problem deals with multiple objectives of a conflicting nature. The objective functions are usually related to the technical performance of the system or cost-related parameters. Therefore in the current study, the problem is one of minimizing purchased electricity and investment costs.

3.2. Objective functions

In this study, purchased electricity and investment costs (IC) are set as objective functions to be minimized. The motivation to use purchased electricity and the investment costs (IC) are of primary interest because purchasing electricity and operational costs (and environmental issues in general) are of interest to the end user and the investment cost is of interest to the contractor. Furthermore, most of the companies building such systems are interested in the investment cost of the system rather than the operational cost. Therefore it is important to evaluate all these quantities in order to provide the overall performance of the system.

The two functions that are analyzed are the purchased electricity of the system together with the houses and the investment costs (IC) together. It is given as:

$$\text{Min } \{F1\ (x) = \text{Purchased electricity},\ F2(x) = \text{investment costs (IC)}\},, \text{ for all } x = [x_1,\ x_2,\ \ldots, x_n],$$

where 'x' is the vector of the design variables $(x_1, x_2, \ldots, x_n)$ as defined in Subsection 3.3, F1 is the purchased electricity for the system together with the houses, and F2 is the investment costs (IC) of the system. In this problem, the number of considered design variables are six (i.e., $x = [x_1, x_2, \ldots, x_6]$).

The mathematical expression for purchased electricity is,

$$E_{PUR} = E_{PUMP} + E_{HP} + E_{BH} + E_{BUL} - E_{EXP}, \quad (1)$$

where E_{PUR} is the purchased electricity, E_{PUMP} is the energy consumed by all pumps, E_{HP} is the heat pump energy consumed to heat the tanks, E_{BH} is the energy use of the direct electric backup heating (used to maintain the temperature in the space heating and

domestic hot water network in case the heat pump and solar energy are not sufficient), E_{BUL} is the appliance electricity demand of buildings, and E_{EXP} is the excess electricity that is produced by PV panels and exported.

The second function – investment costs – is the sum of the present value of the investment cost of the system. It is expressed as

$$IC = C_{ST} + C_{PV} + C_{BTES} + C_{WT} + C_{HT} + C_B, \quad (2)$$

and,

$$C_B = C_{Wins} + C_{Rins} + C_{Fins} + C_{WIND} + C_{HR}, \quad (3)$$

where *IC* is the overall investment cost, C_{ST} is the solar collectors, C_{PV} is the photovoltaic, C_{BTES} is the borehole, C_{WT} is the warm tank, C_{HT} is the hot tank, and C_B is the building costs. The C_B is the building investments, which includes the cost of the building's insulation material, wall (C_{Wins}), roof (C_{Rins}), and floor (C_{Fins}), and the cost of windows (C_{WIND})and building heat recovery (C_{HR}) (Rehman et al., 2017). No maintenance costs are considered. Due to the long simulation calculation time, a five-year simulation is not feasible. Therefore, as a compromise, the system is simulated for three years and used for estimating the performance of the system. Three to five-years simulations are needed because the BTES average temperature becomes steady and change in temperature is not significant in the following years.

3.3. Design variables

The performance of the energy system described in Section 2 mostly depends on the six design variables that are defined and considered in this paper, namely: (1) the ST collector area, (2) warm short-term storage tank volume, (3) hot short-term storage tank volume, (4) BTES volume, (5) the photovoltaic area, and (6) the building's heating demand.

The values or range of the design variables are shown in Table 1. The investment cost of design variables are also shown in Table 1. It is computationally expensive to explore all designs. Hence, a multi-objective non-dominated sorting genetic algorithm (NSGA-II) is used to perform the exploration (Hamdy et al., 2013).

3.4. Simulation environment

A 100-house community is studied, located in Helsinki, Finland (60.19 N, 24.94 E) (World Geodetic System WGS84 standard, 2012–2016). The system is modeled using TRNSYS Simulation Studio (Solar Energy Laboratory, University of Wisconsin-Madison, 2012), and dynamic simulations are performed with a time step of 0.125 h. TRNSYS (Solar Energy Laboratory, University of Wisconsin-Madison, 2012) Type 1b, Type 543, Type 557a, Type 668, Type 194, and Type 15 are used for solar thermal collectors, buffer tanks, boreholes thermal energy storage (BTES), heat pump, photovoltaic panels, and weather data, respectively (Rehman et al., 2017). Finnish test reference year data is used for weather data (Finnish Meteorological Institute, 2012). The buildings' thermal model is built and simulated in TRNBuild (Solar Energy Laboratory, University of Wisconsin-Madison, 2012), which is a TRNSYS subroutine that is able to generate the thermal loads profile of a building. Each house is a single-story house with a pitched roof tilted at a 20° angle. Three different types of buildings with varying heating demands are selected for the study. Based on the previous study, buildings with heating demands of 25, 37, and 50 kWh/m^2/yr are selected (Rehman et al., 2017). The DHW demand is 45 kWh/m^2/yr, and the electrical appliances' demand is 40 kWh/m^2/yr for all three building types.

3.5. Optimization algorithm

In the present approach, the TRNSYS model and MOBO (a multi-objective building optimizer) are combined to perform the optimization. MOBO (Palonen and Hasan, 2017) is freeware optimization software that can handle both discrete and continuous variables and allows the use of evolutionary and classical optimization algorithms. For this study, the NSGA-II algorithm is selected (Deb et al., 2002). In order to justify its selection, a comparison of NSGA-II with other algorithms is provided in Table 2.

An automatic simulation-based optimization method is performed using the NSGA-II algorithm by combining TRNSYS and MOBO software. It avoids the repetition, keeps all the iterations in an archive, and uses them in a non-dominated sorting process. MOBO uses the NSGA-II algorithm with an initial population of 16 individuals for 100 generations (i.e., $16 \times 100 = 1600$ simulation runs) (Alajmia and Wright, 2014).

4. Optimization results – base case

4.1. Optimal solutions

Fig. 2 shows the relationship between the purchased electricity and the investment costs (IC) of the non-dominated optimal solutions (red points) and also all simulation runs (green points) for the energy system discussed.

The solutions of the Pareto front are called non-dominated solutions (red points). In total there are 153 non-dominated solutions for the energy system. Generally, increased investments reduced the amount of purchased electricity. The solutions on the left side of Fig. 2 are less energy-intensive, whereas solutions on the right side of Fig. 2 are more energy-consuming. The purchased electricity varies from 49 kWh/m^2/yr to 25.9 kWh/m^2/yr, which corresponds to investment costs (IC) from 202 €/m^2 to 624 €/m^2, respectively. It shows that there exists a wide range of optimal solutions. All the points on the Pareto front are optimal points and it is up to the decision makers to choose the point based on their objectives and

Table 1
System configuration variations for the simulations and investment cost of the components used in energy systems.

Design variables	Alternative/values	Prices (€)	References
Solar thermal area (m^2)	500–5000	600-500 €/m^2	(Mauthner and Herkel, 2016; GREENoneTEC Solarindustrie GmbH, 2015)
Warm tank volume (m^3)	50–500	825 €/m^3	(Mauthner and Herkel, 2016; Solar district heating, 2012),
Hot tank volume (m^3)	50–500	825 €/m^3	(Mauthner and Herkel, 2016; Solar district heating, 2012)
BTES volume (m^3)	15000–70000	17.19 €/m^3	(CIT Energy Management AB, EU report, 2011)
PV area(m^2)	500–500	230 €/m^2	(AXITEC Solar, 2016)
Building configurations	Type 1: heating demand = 25 kWh/m^2/yr	15,628€/building	(Hamdy et al., 2011; Hamdy et al., 2013; Haahtela and Kiiras, 2013)
	Type 2: heating demand = 37 kWh/m^2/yr	13,260 €/building	
	Type 3: heating demand = 50 kWh/m^2/yr	12,655 €/building	

Table 2
Comparison of the NSGA-II algorithm with other optimization algorithms (Attia et al., 2013).

Algorithm	Features					
	Single objective	Multi-objective problem	Constrained handling	Handling discrete variables	Handling continuous variables	Parallel computing
NSGA-II	Yes	Yes	Yes	Yes	Yes	Yes
Brute Force	Yes	Yes	No	Yes	Yes	Yes
Random search	Yes	Yes	No	Yes	Yes	Yes
Hooke-Jeeves	Yes	No	Yes	No	Yes	No
OMNI optimizer	Yes	Yes	Yes	No	Yes	Yes

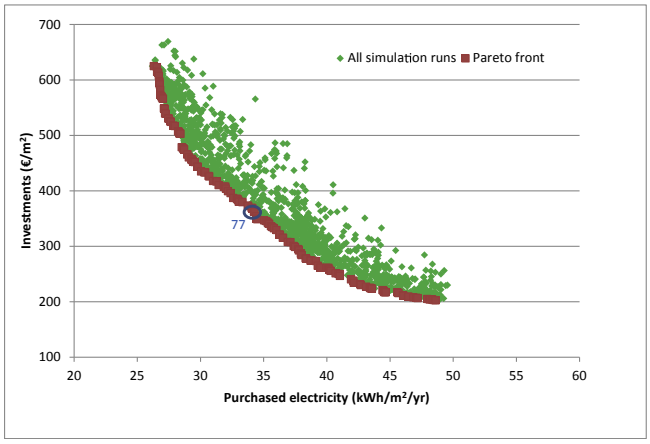

Fig. 2. Purchased electricity versus investments of the non-dominated optimal combinations of the design variables.

criteria. However, the Pareto optimal point that is closest to the ideal point could be interpreted as the single optimal point. The ideal point is a theoretical point where both the objectives are at their minimum values i.e. 25.9 kWh/m^2/yr (x-axis) and 202 €/m^2 (y-axis). The single optimal point is therefore point 77, shown in Fig. 2. The corresponding values of the purchased electricity is 34 kWh/m^2/yr and investments cost is 367 €/m^2 at this point on the Pareto front.

The left-most points of the Pareto front contained solutions with a large solar thermal area. In contrast, the right-most points of the Pareto front contained solutions with a small solar thermal area. It was found that the discontinuous behavior or two gaps on the Pareto front is caused by the changing of the building type.

4.2. Analysis of the non-dominated solutions

Fig. 3 shows the cost breakdown of the non-dominated optimized solutions for the energy system.

The solutions on the left side of Fig. 3 are the expensive solutions; however the purchased electricity is lowest for these solutions. On the other hand, the solutions on the right side are the least expensive solutions; while, the purchased electricity is highest.

Fig. 3 show that the solar thermal area played a significant part in the investments. Hence, due to the higher cost, a smaller collector size is chosen in the least expensive solutions. On other hand, larger sizes of the ST improved the system performance by reducing the purchased electricity.

Buildings with a high heating demand are selected for 40 solutions. But, buildings with the smallest heating demand are subsequently selected in all other cases. It again indicates that building heating demand played an important role in varying and improving system performance. Due to the slight difference in the cost among the buildings, the algorithm's first option is to change the building from higher to lower heating demand buildings in optimized cases.

Furthermore, the warm tank volume also increased gradually from the least expensive to the most expensive solution. This again indicates that large a warm tank volume would improve the performance of the system. This would improve the availability of the instantaneous low temperature energy available for the system to meet the demand.

The solutions on the left side of Fig. 3 shows that a combination of medium to large ST area, large warm tank volume, energy-efficient building, and medium size of the BTES volume could improve the performance in Finnish conditions. This would also increase the investments. On the other hand, a combination of small ST, energy-efficient building, medium-sized warm tank, smaller BTES volume, and larger PV area can provide a medium-ranged performance of the system with fewer investments. The renewable energy fraction varied from 65 to 90%. The solution 96 showed slight decrease in the fraction due to change in the building heating demand by the NSGA-II algorithm.

5. Influence of system failures and defects

5.1. Selected failures and defects

The novelty of this paper is to introduce reported experiences from implemented solar district heating systems and computationally investigate their influence on some selected optimized system configurations. This makes it possible to analyze the effect of non-ideal conditions on the performance of the proposed optimized system.

In general, the energy performance of the energy system is sensitive to various technical parameters, as explained in many earlier studies (Hakaste et al., 2008; Faninger-Lund, 2003; Ochs et al., 2008; Dalenbaeck, 1998; Nielsen, 2012; Truong and Gustavsson, 2014; Boyaghchi et al., 2015). In addition, the significance and nature of these parameters can be different for varying systems. Some of the most common parameters that can alter the system performance in real conditions which are defined and considered in this paper are: (1) heat exchanger efficiency, (2) solar thermal collector intercept efficiency, (3) tank stratification, (4) annual average heat pump coefficient of performance (COP), (5) space heating(SH) network temperature difference, (6) hot tank set points, (7) warm tank set points, (8) space heating(SH) supply temperature, (9) solar thermal circulation pump, and (10) thermal conductivity of boreholes boundary. The details along with the results of each parameter are described in Section 5.2.

For the base case, these parameters are considered to be state-of-the-art values when the system is performing well and based on designed optimized values. For the other cases, these ten parameters are altered in a way that the system is underperforming and its performance is compared to the base case. The base case value and the altered scenario values are shown in Table 3. From the literature, there are no clear hints as to the amount of defects or failures for every technical parameter. Therefore, the amount of

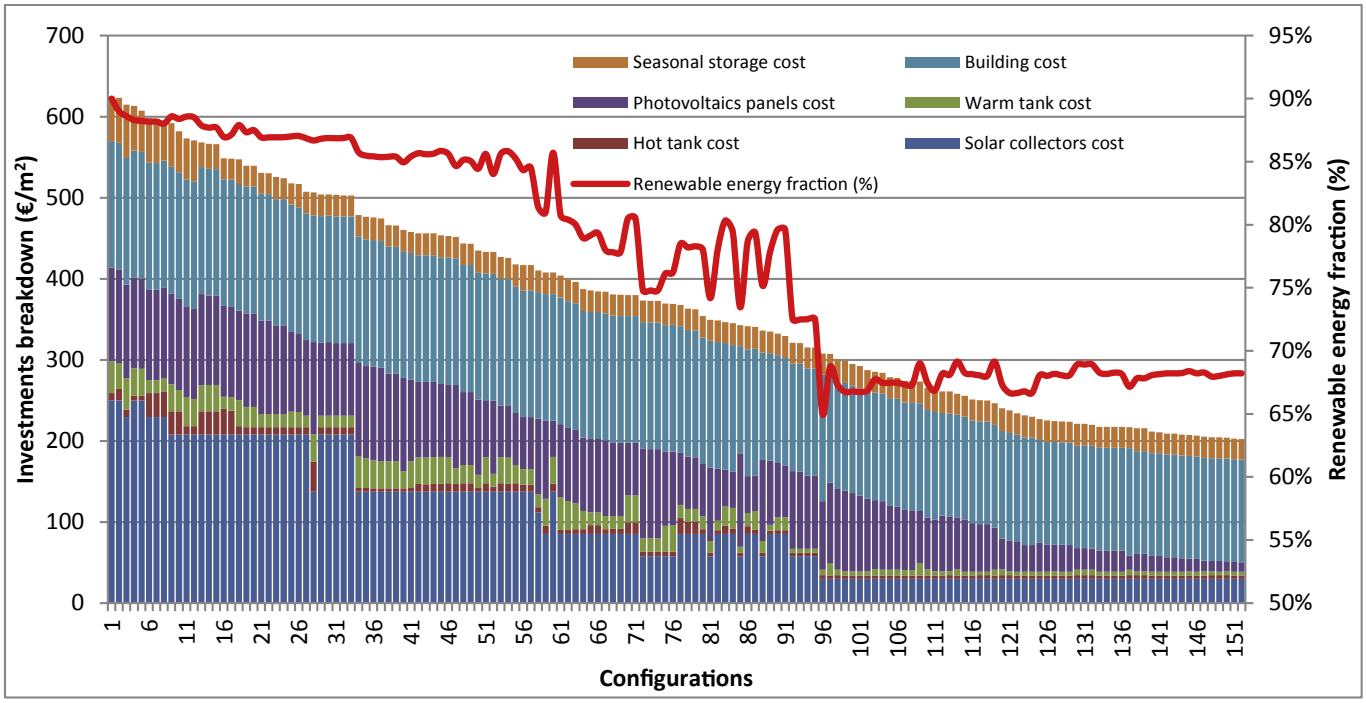

Fig. 3. The cost breakdown of the non-dominated optimal solutions.

Table 3
Technical parameters considered for the system performance deviations.

Technical parameters	Values before defects (optimized case)	Values after defects (deviation case)	References
Heat exchanger efficiency	0.9	0.7	(Hannoschöck, 2016; Lundh and Dalenbäck, 2008; Dincer and Rosen, 2007)
Solar collector intercept efficiency	0.9	0.7	(ESTIF - the European Solar Thermal Industry Federation, 2006; Nussbicker-Lux, 2012)
Tank stratification	Stratified	Fully mixed	(Koppen et al., 1979; Sibbitt et al., 2012)
Heat pump (COP)	5–6	3–4	(NIBE, 2017; Nussbicker-Lux, 2012)
SH temperature difference	7-3 °C	5-1 °C	(Ministry of the Environment, Department of the Built Environment, 2010; Nussbicker-Lux, 2012; Dincer and Rosen, 2007; Rehman et al., 2017)
Hot tank set point	70 °C	75 °C	(Nussbicker-Lux, 2012; Rehman et al., 2017)
Warm tank set point	45 °C	50 °C	(Nussbicker-Lux, 2012; Rehman et al., 2017)
SH supply set point	40-30 °C	50-40 °C	(Ministry of the Environment, Department of the Built Environment, 2010; Nussbicker-Lux, 2012; Dincer and Rosen, 2007; Lundh and Dalenbäck, 2008)
Solar thermal circulation pump	Variable pump circulation control	On/off pump circulation control	(Sibbitt et al., 2011)
Thermal conductivity of boreholes boundary layer	3.5 W/m.K	4.5 W/m.K	(Tordrup et al., 2017; Hakala et al., 2014)

defects for each parameter is assumed in a reasonable range to exhibit real scenarios. From Fig. 3 configuration number 1, 12, 55, 77, 96, 121 and 153 were chooses as base case (optimized) and they are further referred as cases 1, 2, 3, 4, 5, 6 and 7 respectively in the following text and failure cases.

5.2. Influence of failures and defects on the system performance – results and discussion

5.2.1. Heat exchanger efficiency

Heat exchanger is an important mechanical device used in the energy system. Heat exchangers are used between the collectors, short term storage tanks and district heating network. Heat exchanger efficiency is defined as the ratio of the heat transferred in the actual heat exchanger to the heat that would be transferred in an ideal heat exchanger. Efficiency is a comparison between the actual (real) and ideal (best) performances and is typically defined as being less than 1, or at best, equal to 1. The ideal behavior is generally known from modeling and the limitations dictated by physical laws, particularly the second law of thermodynamics (Fakheri, 2006). The typical efficiency of the water to water plate type heat exchanger can be higher than 0.9 (Hannoschöck, 2016). It is assumed that due to the failure and defects, the overall heat exchanger efficiency drops by 22% from 0.9 to 0.7.

Heat exchanger efficiency affects the overall performance of the system, as shown in Fig. 4. Due to the reduction in heat exchanger efficiency, the selected optimal points of the base case (blue points) shifted towards the right (red points). The shift is around 3–4% due to the increase in the purchased electricity caused by the reduction in heat exchanger efficiency.

The fouling of the heat exchanger surface led to a reduction in the transfer of solar heat from the solar net to the tanks and from the tanks to the district heating net. This caused very high temperatures in the collector circuit and thus reduced collector

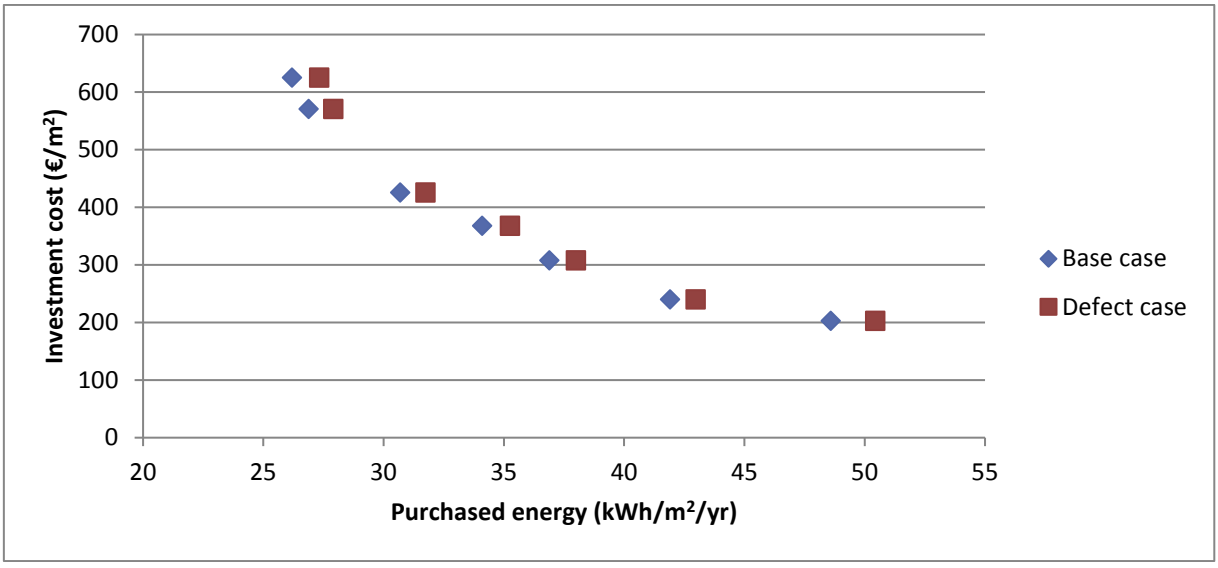

Fig. 4. Purchased electricity versus investments deviation caused by the change in heat exchanger efficiency.

efficiency. This fault changed the solar collector energy production around 5% (Fig. 5). The range of renewable energy fraction is reduced from 65 to 90% (base case) to 52–83%.

5.2.2. Solar thermal collector intercept efficiency

The efficiency of solar thermal collectors varies depending on the solar radiation, outside temperature, and collector fluid temperature. Efficiency is not a constant – it depends strongly on the temperature difference between the collector and the outside air (Build it solar, 2006). The intercept efficiency is the efficiency is a point on the efficiency curve when there is no difference between the collector temperature and ambient temperature (Struckmann, 2008). The flat plate solar thermal collectors have a typical intercept efficiency of approximately 0.9 (ESTIF - the European Solar Thermal Industry Federation, 2006). The common reasons for the performance degradation is the fouling inside the collectors, dirt accumulation on the surface, trapped air (air lock) in the collectors, and the aging of the collectors. In Friedrichshafen, the solar thermal efficiency in the first year could not be repeated in the following years (Bauer et al., 2010) due to degradation. In this study, it is assumed that due to the failure and defects, the overall intercept efficiency point shifts by 22% down to 0.7. The relative shift in the purchased energy caused by failures and defects are mentioned in Table 4 and all results are referred to Table 4 in all further failure scenarios. This fault changes the range of purchased electricity from 25.9 kWh/m^2/yr – 49 kWh/m^2/yr to 27.3 kWh/m^2/yr – 50.4 kWh/m^2/yr. The shift is due to the increase in the purchased electricity caused by the reduction in the solar thermal collector efficiency.

Fig. 6 shows the reduction in solar yield by the collectors. The reduced useful energy gain by the working fluid reduced the transferred energy to the storage tanks compared to perfectly efficient solar collectors. This fault changed the solar collector energy production about 12%–25% (Fig. 6). The range of renewable energy fraction is reduced from 65 to 90% (base case) to 62–86%.

5.2.3. Tank stratification

The buffer tanks are the most important part of the stratified TES system. Stratification is just a natural process: the warmth and density of water are inversely proportional properties. It is found that stratification allows low temperature working fluid to enter at the collector inlet, which increases its efficiency (Koppen et al., 1979; Furbo and Mikkelsen, 1987). Although stratified TES is inexpensive, there are still problems with low energy density and complexity in designing the storage tanks (ARANER, 2016). Due to

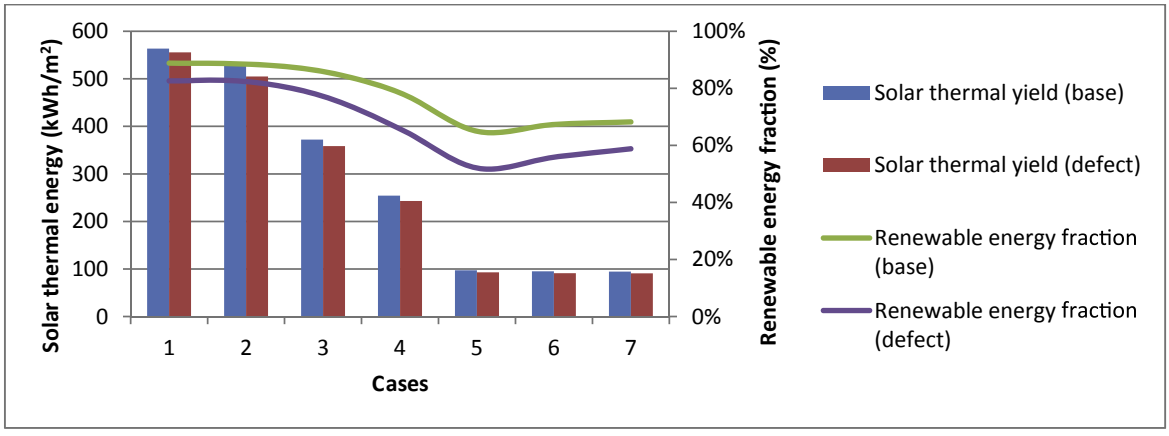

Fig. 5. Solar thermal yield and renewable energy fraction deviation caused by the change in heat exchanger efficiency.

Table 4
Purchased electricity relative increase caused by various failures.

Technical parameters	Case 1	Case 2	Case 3	Case 4	Case 5	Case 6	Case 7
Heat exchanger efficiency (5.2.1.) - Relative value (%)	4%	4%	3%	3%	3%	3%	4%
Solar thermal collectors intercept efficiency (5.2.2.) - Relative value (%)	9%	8%	8%	4%	3%	3%	2%
Tank stratification (5.2.3.) - Relative value (%)	34%	34%	34%	35%	30%	29%	23%
Annual average heat pump coefficient of performance (5.2.4.) - Relative value (%)	7%	8%	9%	13%	19%	20%	21%
Space heating temperature difference (5.2.5.) - Relative value (%)	4%	4%	4%	5%	3%	3%	3%
Hot tank charging set point temperature (5.2.6.) - Relative value (%)	5%	4%	4%	6%	3%	3%	3%
Warm tank charging set point temperature (5.2.7.) – Relative decrease in value (%)	1%	1%	1%	3%	3%	3%	2%
Space heating supply temperature set point (5.2.8.) - Relative value (%)	3%	2%	3%	6%	5%	5%	6%
Solar thermal collector circulation pumps control (5.2.9.) - Relative value (%)	22%	17%	8%	2%	1%	1%	1%
Thermal conductivity of boreholes boundary layer (5.2.10.) - Relative value (%)	7%	6%	4%	3%	3%	3%	3%

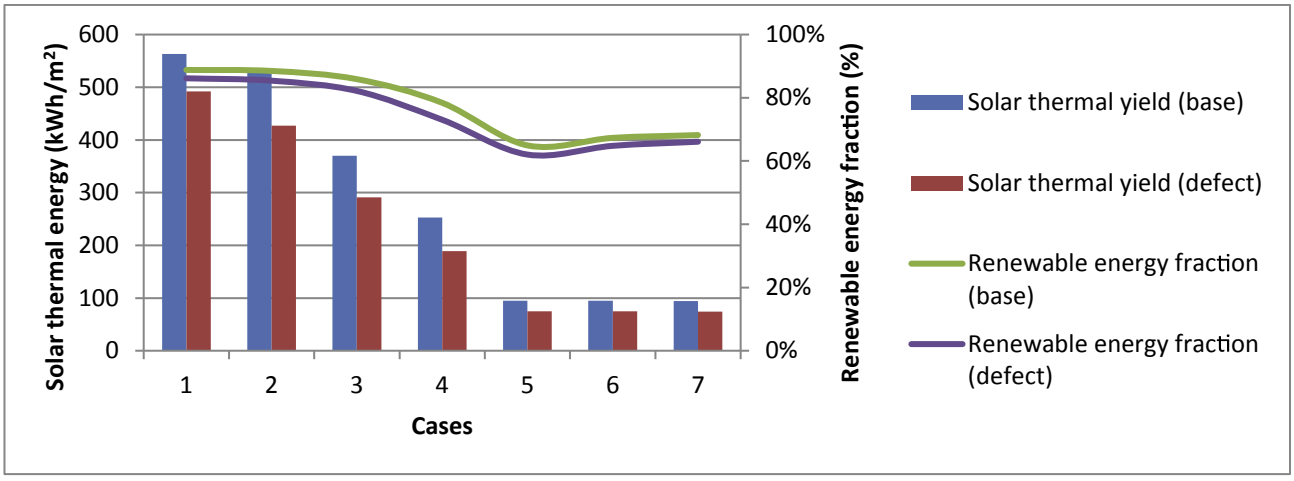

Fig. 6. Solar thermal yield and renewable energy fraction deviation caused by the change in solar thermal collector intercept efficiency.

flow variations, wrong internal tank design and nodes distribution can cause loss of stratification.

In this study, the simulated tanks are divided into 5 equally spaced nodes vertically, and the temperature gradient between the top and bottom of the tank is 10 °C in the stratified condition. The stratified cases are compared to cases where the storage tanks are fully mixed and there is only a single temperature node. Due to the loss of stratification, the optimized points shifted in each case. The shift is due to the reason that the lowest temperature is not available for the collection of heat energy from the solar collectors. This fault increases the range of purchased electricity from 25.9 kWh/m^2/yr – 49 kWh/m^2/yr to 35.1 kWh/m^2/yr – 60.1 kWh/m^2/yr.

Due to the high supply temperature in the solar collector circuit, the efficiency of the collectors is reduced. Fig. 7 shows the reduction in the solar yield by the collectors due to the high temperature in the collector circuit. Therefore it is important to maintain the stratification in the tanks in order to provide a low temperature inside the collector circuit. Heat losses from tanks, pipes, and boreholes are increased due to the high temperature. This causes an increase in the backup heating and heat pump energy needs due to losses through pipes. This fault cuts the solar collector energy production around 5% in Fig. 7. The range of renewable energy fraction is reduced from 65 to 90% (base case) to 36–77%.

5.2.4. Annual average heat pump coefficient of performance (COP)

The efficiency of heat pumps is denoted by its Coefficient of Performance (COP). The COP is determined by the ratio between the amount of useful heat extracted from the condenser and energy usage of the compressor. A high COP value represents high efficiency. For a certain compressor the temperature difference between condensation and evaporation temperature mainly determines the efficiency: the smaller the difference, the higher the COP. The COP of the applied HP is 5–6 (NIBE, 2017), depending on the BTES and the desired output temperature. The COP of the HP used in the simulation is reduced by around 30% so that the new COP of the HP is 3–4. Due to the heat pump COP reduction, the selected optimal points shifted in each case. This failure diminished the range of purchased electricity from 25.9 kWh/m^2/yr – 49 kWh/m^2/yr to 28.1 kWh/m^2/yr – 61.1 kWh/m^2/yr.

The most common failure with a heat pump might be in the controls. The use of heat pump is not maximised and the aux heater is too much in use. Fig. 8 shows the reduction in solar yield by the collectors. Due to inefficient performance, the heat pump is not able to utilize all of the heat present in the warm tank, hence the solar yield is reduced. This fault changed the solar collector energy production around 3% (Fig. 8). The decrease in the COP of the heat pump caused an increase in the need for backup heat energy. The range of renewable energy fraction is reduced from 65 to 90% (base case) to 48–85%.

5.2.5. Space heating temperature difference

The space heating network plays an important role in the overall system performance. In most of the heating networks, it is always recommended to have a higher temperature difference between the supply and the return temperature so that the return temperature is as low as possible. This improves the efficiency of the power or heating plant (Urbaneck et al., 2015; Bauer et al., 2016; BINE Information Service, 2000). However, it is found that most of the plants faced the issue of a higher return temperature in the district heating network (Ministry of the Environment, Department of the

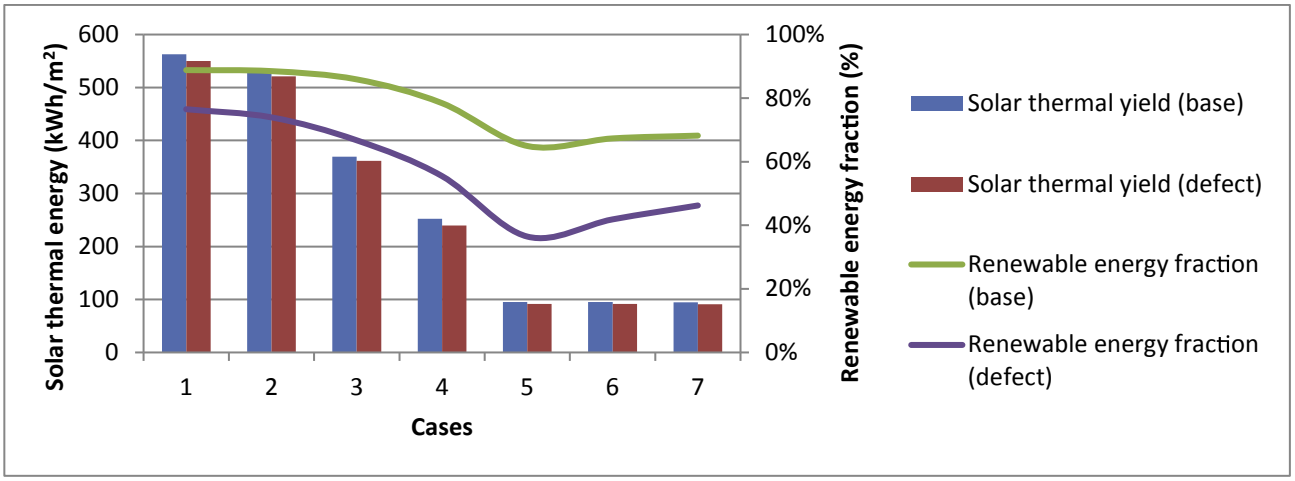

Fig. 7. Solar thermal yield and renewable energy fraction deviation caused by the stratification issues.

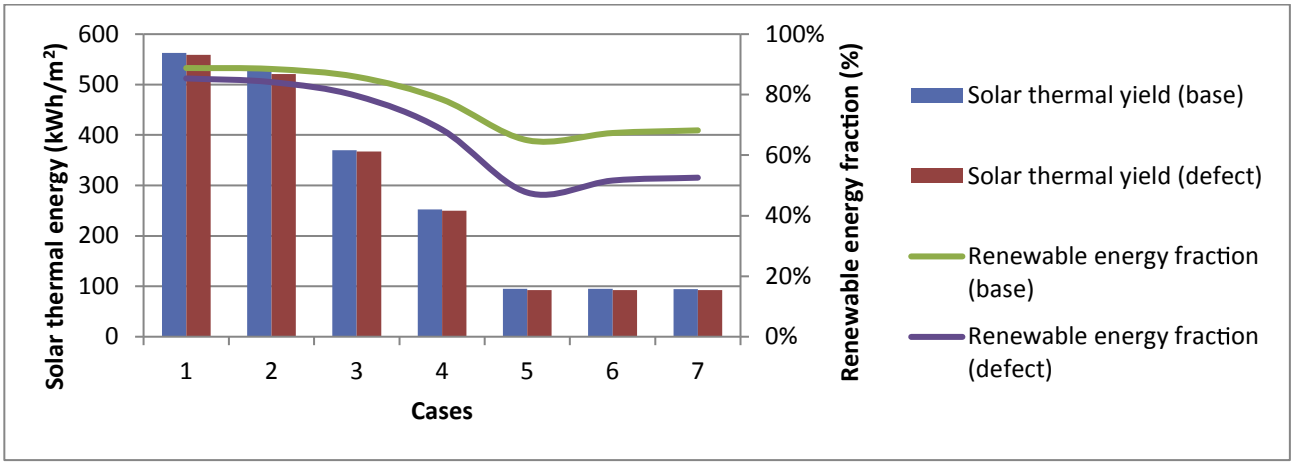

Fig. 8. Solar thermal yield and renewable energy fraction deviation caused by the change in the annual average heat pump coefficient of performance (COP).

Built Environment, 2010; Nussbicker-Lux, 2012; Dincer and Rosen, 2007; Rehman et al., 2017; Sibbitt et al., 2011). Therefore, the temperature difference between the supply and return temperature decreases. In the current configuration, the temperature difference range between the supply and return space heating network temperature is set at (7-3 °C) (Rehman et al., 2017), depending upon the space heating supply temperature. This temperature difference range was reduced by 2 °C so that the range is (5-1 °C). Due to the reduction in the temperature difference between the supply and return space heating network, the selected optimal points shifted in each case. This malfunction increased the range of purchased electricity from 25.9 kWh/m^2/yr – 49 kWh/m^2/yr to 27.2 kWh/m^2/yr – 50 kWh/m^2/yr.

The main reasons for the higher return temperature are wrong design in the building heating system, HVAC, and district network. This causes the return temperature to be higher than the design temperature. The higher temperature increases the temperature in the warm tanks, and this higher temperature in the tanks causes a reduction in the collector performance. Since the return temperature is higher, the heat exchange between the tanks and space heating network is not efficient. This fault caused a deviation in the solar collector energy production of about 6% in Fig. 9. The range of renewable energy fraction is reduced from 65 to 90% (base case) to 63–87%.

5.2.6. Hot tank charging set point temperature

In the current configuration, the temperature set point of the hot tank is at 70 °C (Rehman et al., 2017) when charging via ST collectors. This set point temperature is increased by 5 °C such that the set point is now 75 °C. This is done to replicate the issue of a control malfunction. Table 4 shows that when a higher charging set point temperature is used, it resulted in a slight increase in the purchase electricity. It also increased the losses in the tanks and the district heating network piping. This malfunction caused a slight deviation in the range of purchased electricity from 25.9 kWh/m^2/yr – 49 kWh/m^2/yr to 27.5 kWh/m^2/yr – 50.1 kWh/m^2/yr.

The main reasons for the change in the tank charging set point temperature is a malfunction in the control or an error in the control algorithm or device. This causes a change in the set point. The higher temperature in the tank reduced the solar thermal yield due to the higher supply temperature for the solar thermal collectors. Fig. 10 show this error changed the solar collector energy production by about 8%. This caused an increase in the backup heating and heat pump energy need due to losses through pipes. The range of renewable energy fraction is reduced from 65 to 90% (base case) to 65–87%.

5.2.7. Warm tank charging set point temperature

The warm tank charging set point plays an important part in the

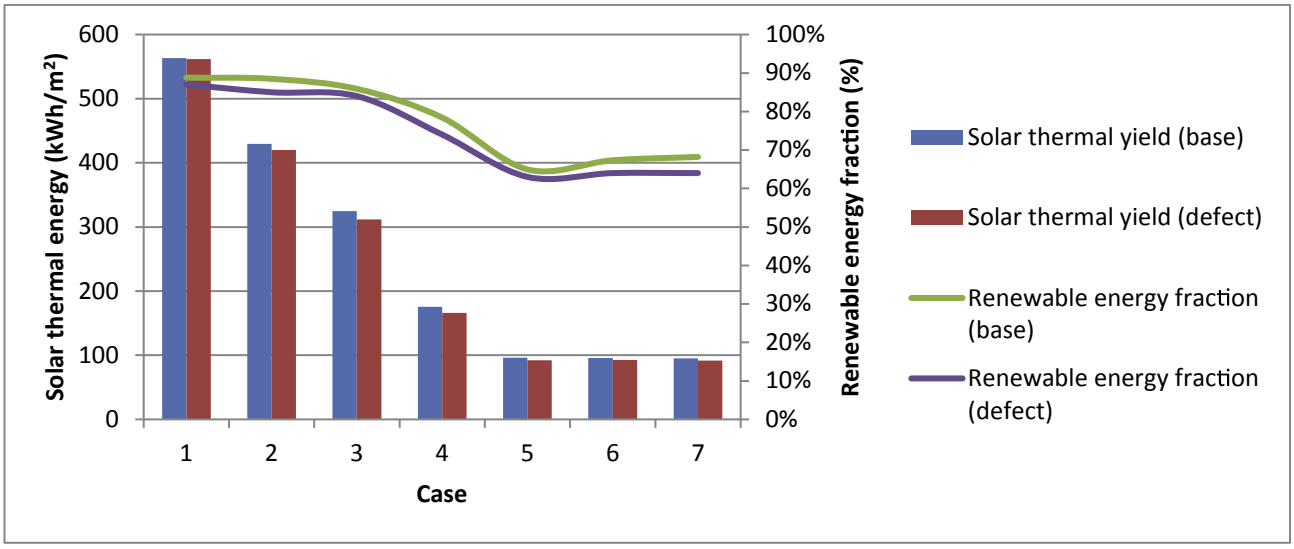

Fig. 9. Solar thermal yield and renewable energy fraction deviation caused by higher return temperature.

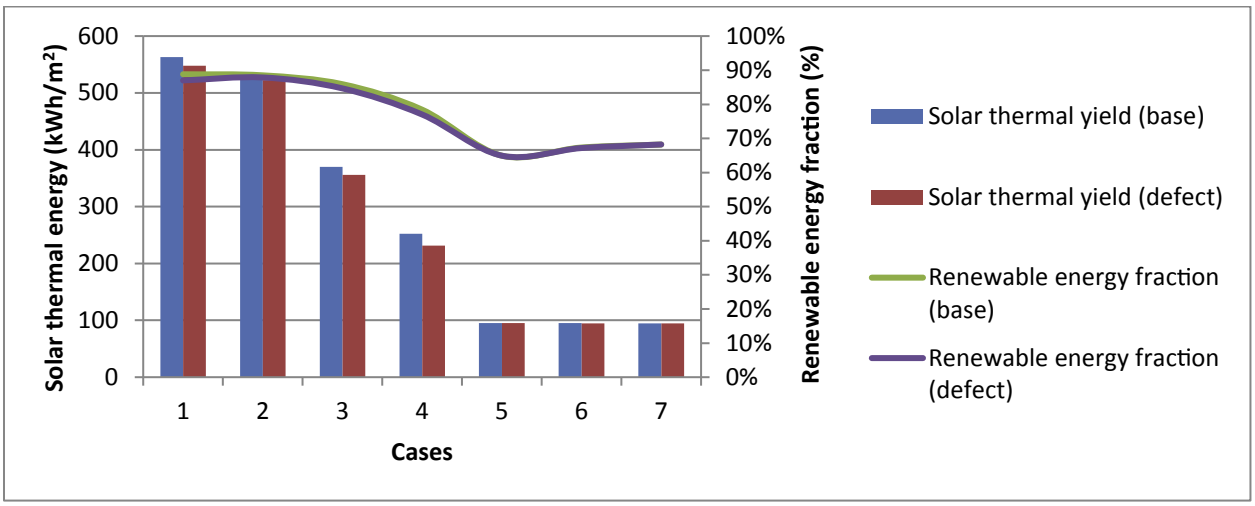

Fig. 10. Solar thermal yield and renewable energy fraction deviation caused by a higher hot tank charging set point.

overall system performance. In the current configuration, the temperature set point of the warm tank is increased by 5 °C (similar to sub-section 5.2.6). It is found that, it improved the performance of the system, as there is a slight decrease in the purchased electricity. The decrease in the purchased electricity is due to higher temperatures in the tank, which can provide better preheating of the SH and DHW water before it enters the hot tank for final temperatures. This defect slightly reduced the range of purchased electricity from 25.9 kWh/m^2/yr – 49 kWh/m^2/yr to 25.5 kWh/m^2/yr – 48.1 kWh/m^2/yr.

The higher temperature in the tank reduced the solar thermal yield due to the higher supply temperature for the solar thermal collectors similar to Fig. 10. This fault changed the solar collector energy production by about 2%. Due to a slight improvement in the performance, the range of renewable energy fraction changed from 65 to 90% (base case) to 68–89%.

5.2.8. Space heating supply temperature set point

As discussed above in Section 5.2.5, the space heating network plays a significant part in the overall system performance. The increase in the supply temperature can happen due to a malfunction in the control algorithm or control system. One of the issues found in the plants (Urbaneck et al., 2015; Bauer et al., 2016; BINE Information Service, 2000) that causes deviations in the plant performance is the space heating network temperature. Although in Finland the space heating network supply temperature varies from (40-30 °C) in floor heating systems (Ministry of the Environment, Department of the Built Environment, 2010; Rehman et al., 2017), depending on the ambient temperature. In this scenario, the supply temperature is increased to (50-40 °C) based on the supply set point used in Drake Landing Solar Community, Canada (Sibbitt et al., 2015). Due to the increase in the space heating supply temperature, the selected optimal points shifted in each case. The increase in the set point causes an increase in the backup heating demand, a higher return temperature from the district heating network, and an increase in losses through pipes. This fault changed the range of purchased electricity from 25.9 kWh/m^2/yr – 49 kWh/m^2/yr to 26.9 kWh/m^2/yr – 51.3 kWh/m^2/yr.

The main reason for the supply temperature set point is a wrong

design in the control system or a malfunction in the controls. This causes the supply temperature to be higher than the designed temperature. The higher temperature increases demand of the backup heating and the heat pump energy. Furthermore, the space heating network return temperature also increases. This fault changed the solar collector energy production by around 4% (Fig. 11). Corresponding to the solar thermal yield, heat loss through the district heating piping network increased from 13% (base case) to 16%. This also causes an increase in the backup heating and heat pump energy needs due to losses through pipes. The range of renewable energy fraction is reduced from 65 to 90% (base case) to 61–87%.

5.2.9. Solar thermal collectors circulation pump control

The solar thermal circulation pump control plays a significant part in overall system performance. In Drake Landing Solar Community, Canada (Sibbitt et al., 2011), variable speed drives are employed to power the collector loop pumps to minimize electrical energy consumption while handling a wide range of thermal power levels. Typically, during the early morning hours, evenings, and during low solar irradiation periods, heat cannot be extracted from the solar thermal collectors field quickly enough at higher temperature to meet heat demands. Therefore the flow through the collectors is reduced or adjusted to provide the set point temperature to the tanks in need. The current setup allows the pump flow to be adjusted and varied based on the set point of the tank and the collector inlet temperature. Hence the pump does not operate at full power or zero power, and this avoids the fluctuation (On/Off) condition. A defect can arise in the control, which can cause a malfunction in the control algorithm or control system of the collectors pump. This malfunction can result in the continuous operation of the pump, which is either on or off. The maximum flow rate of the pump is based on the collectors area, i.e., the larger the area, the larger the flow rate. In this case, the increase in the flow rate (at continuous full flow) causes an increase in the purchased electricity. The losses through the collectors caused cooling of the tanks due to low temperature fluid entering the tanks. This fault changed the range of purchased electricity from 25.9 kWh/m^2/yr – 49 kWh/m^2/yr to 31.9 kWh/m^2/yr – 50 kWh/m^2/yr. It is found that the effect of error is large in the case where solar thermal area is larger. The larger ST area tends to have a larger effect and deviation because it has larger flow rates, higher temperatures, and more ST area to lose energy.

The assumed reason for the change in the pump variable drive is the malfunction in the control or error in the control algorithm or device. This causes the pump to operate at full power. Since the pump operates at full power and the flow is not varied based on the collectors outlet temperature and tank set points, the pump draws hot fluid from the charged tanks, and this high temperature fluid energy is lost through the collectors in the environment during low irradiation periods. This results in reduction of the solar thermal yield. A fault in the pump control changed the solar collector energy production around 4–12% in Fig. 12. The range of renewable energy fraction changed from 65 to 90% (base case) to 52–73%.

5.2.10. Thermal conductivity of boreholes boundary layer

Dimensioning of large-scale borehole thermal energy storage (BTES) is inherently uncertain because of natural variation in thermal conductivity and heat capacities of the ground. However, practical experiences from existing BTES systems demonstrate different levels of success. BTES in Annenberg (Sweden) (Tordrup et al., 2017), in Attenkirchen and Crailsheim (Germany) (Mangold and Schmidt, 2003), and in Torino (Italy) (Tordrup et al., 2017) showed variations in the performance due to variations in the BTES conductivity. Therefore, in case of highly fractured rock or large fractures intersecting the rock volume, the ground water transported in the fracture may cause significant heat loss from the storage. In Finland, the mean thermal conductivity of rocks is 3.5 W/m.K (Honkonen, 2016). The thermal response tests carried out in Finland showed that the ground conductivity can be as high as 4.5 W/m.K in the presence of water (Hakala et al., 2014). Hence, this value was used to estimate the performance and the reduction in the performance of the energy system. Due to the increase in the thermal conductivity of the BTES boundary (caused by groundwater flow), the selected optimal points shifted in each case. This defect increased the purchased electricity range from 25.9 kWh/m^2/yr – 49 kWh/m^2/yr to 28.1 kWh/m^2/yr – 50.1 kWh/m^2/yr.

The main reason for the increase in the overall effective thermal conductivity is due to the ground water flow through the rocks fracture. The higher conductivity of the BTES increases the losses from the BTES to the surroundings. It is found that average BTES efficiency reduced from 32% (base cases) to 30%. Due to an increase in the losses from the BTES, the solar yield increased by 2% compared to the base case as shown in Fig. 13. This increase in yield is caused by low temperature water availability for the system to collect more solar energy from the collectors. But due to an increase in the losses, this additional solar yield is wasted in the environment, causing an overall decrease in the system performance. The range of renewable energy fraction is reduced from 65 to 90% (base case) to 63–86%, as shown in Fig. 13.

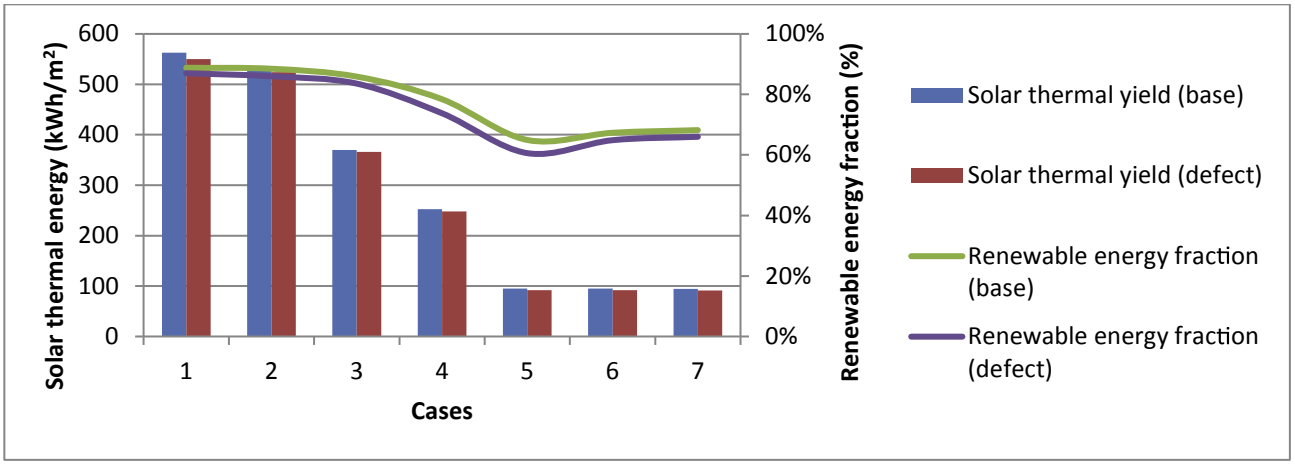

Fig. 11. Solar thermal yield and renewable energy fraction deviation caused by a higher space heating supply temperature set point.

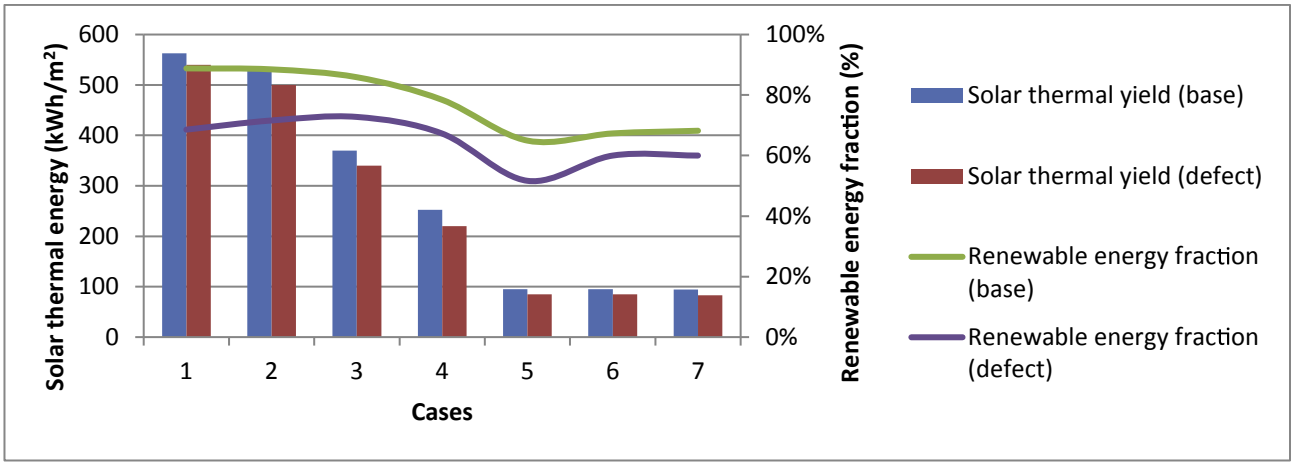

Fig. 12. Solar thermal yield and renewable energy fraction deviation caused by continuous operation of the solar collector circulation pump.

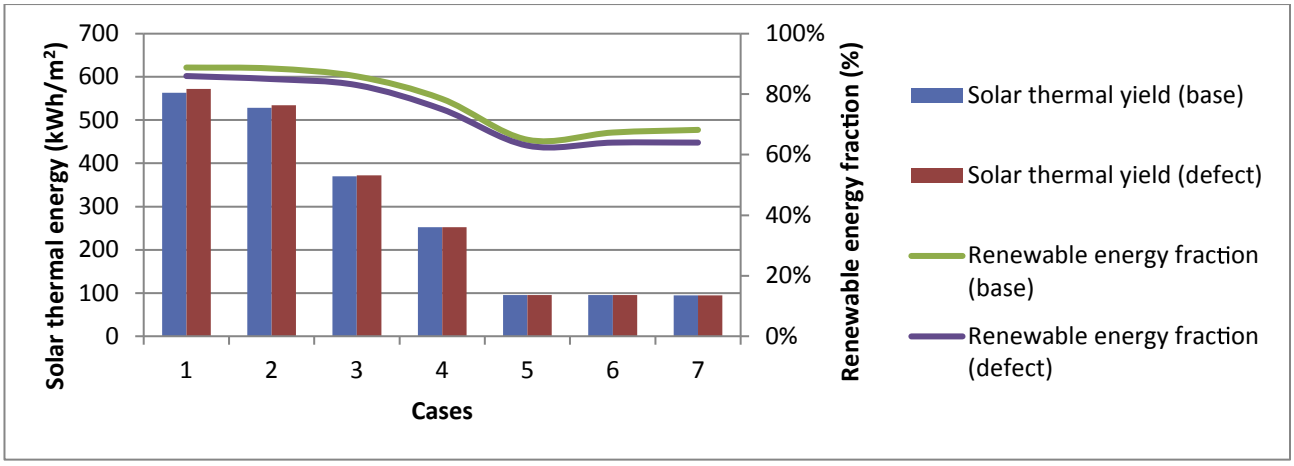

Fig. 13. Solar thermal yield and renewable energy fraction deviation caused by change in the thermal conductivity of boreholes boundary layer.

Table 4 provides an overall summary of the defects and thus the deviations in purchased electricity caused by those defects and failures. The relative changes in the values compared to the optimized base cases are shown.

Generally it is found in Table 4 that, in high performance cases (cases 1) slight technical failures can cause large increase in the purchased electricity, when the solar thermal area is large along with energy efficient buildings compared to the cases 7. On the other hand, in the least performance cases (cases 7), only in the failures like reduction in heat pump COP and increase in the space heating supply temperature set point. The increase in the purchased electricity is slightly large, when the solar thermal area is small along with less energy efficient buildings, compared to cases 1. Therefore, it is essential to know that the collectors area and building heating demand coupled with the technical failures can play significant role in relative increase in the purchased electricity.

5.3. Influence of combined failure effect on system performance

Discussed previously in Section 5.2, it was found that every design variable of the solar thermal system played a part in the overall system performance, though some are clearly more influential than others. In order to analyze the performance of the energy system under the combined effect of all the design variable failures, all the variables are altered from the base case together, although the occurrence of this kind of combined failure probability is quite low. However, this is chosen as the worst-case scenario. The variables that are altered together and simulated are: (1) heat exchanger efficiency, (2) solar thermal collector intercept efficiency, (3) tank stratification, (4) annual average heat pump coefficient of performance (COP), (5) space heating (SH) network temperature difference, (6) hot tank set points, (7) warm tank set points, (8) space heating (SH) supply temperature, (9) solar thermal circulation pump, and (10) thermal conductivity of boreholes boundary. Fig. 14 shows that due to the increase in the set points of controls and reduction in the components performance caused an increase in the backup heating demand, heat pump electricity demand, and losses through the district heating network. These faults and defects caused a deviation in the value of purchased electricity from 150% compared to the base case in Fig. 14.

The main reasons for the deviation of the design variable from the base case can be wrong design in the control system, heating system equipment, maintenance issues, malfunctioning of control devices, and wrong sizing of the HVAC and district network. It is possible that multiple issues can exist at the same time. This could have a domino effect – when one event sets off a chain of similar events. Therefore, the overall performance would reduce drastically. These faults and defects changed the solar collector energy production around 50% (Fig. 15). The range of renewable energy fraction reduced from 65 to 90% (base case) to 0.01–15%.

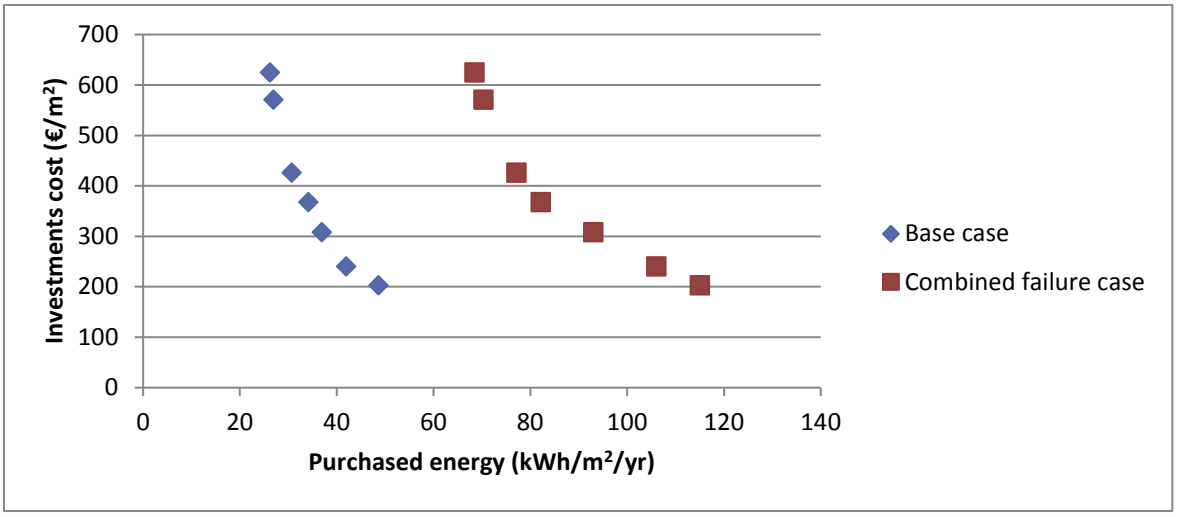

Fig. 14. Purchased electricity versus investment deviation caused by continuous operation of the solar collector circulation pump.

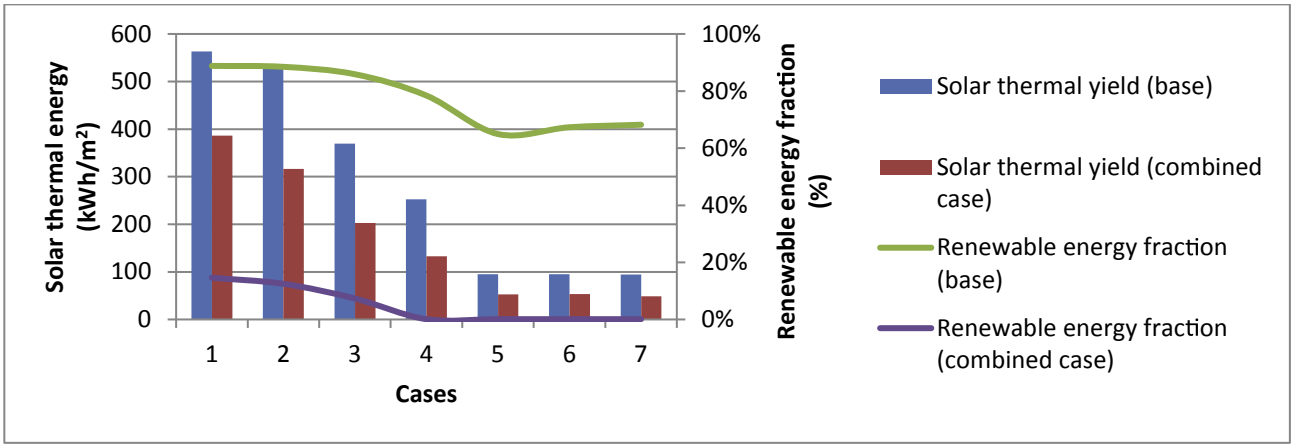

Fig. 15. Solar thermal yield and renewable energy fraction deviation caused by combined failure.

Table 5 provides an overall summary of the defects and thus the deviations in system performance caused by those defects and failures.

Table 5 shows that the following factors have a greater effect on the overall system performance (from highest-to lowest-ranked deviations in purchased electricity): tank stratification, solar thermal circulation pump setting, heat pump COP, solar collectors intercept efficiency, BTES boundary layer thermal conductivity,

Table 5
Overall summary of the defects in the technical parameters, and the deviations in system performance resulting from those defects.

Technical parameters	Values before defects	Values after defects	Increase in purchased electricity	Renewable energy fraction before defects (ideal conditions)	Renewable energy fraction after defects (non-ideal conditions)
Tank stratification	Stratified	Mixed	23 -35%	65-90%	36-77%
Solar thermal circulation pump	Variable pump circulation control	On/Off pump circulation control	1-22%	65-90%	52-73%
Heat pump (COP)	5–6	3–4	7-21%	65-90%	48-85%
Solar collectors intercept efficiency	0.9	0.7	2-9%	65-90%	62-86%
Thermal conductivity of boreholes boundary layer	3.5 W/m.K	4.5 W/m.K	3-7%	65-90%	63-86%
SH supply set point	40-30 °C	50-40 °C	2-6%	65-90%	61-87%
Hot tank set point	70 °C	75 °C	3-6%	65-90%	65-87%
SH temperature difference	7-3 °C	5-1 °C	3-5%	65-90%	63-87%
Heat exchanger efficiency	0.9	0.7	3-4%	65-90%	52-83%
Warm tank set point	45 °C	50 °C	1-3% (Slight reduction in purchased electricity)	65-90%	68-89%(Slight improvement in performance)
Combined failure	Base case	All issues together	150%	65-90%	0.01–15%

space heating supply temperature set point and hot tank charging set point. Only the temperature change of the warm tank set point slightly improved the performance of the system. Therefore, it is important to consider these factors during the design and practical application of a solar thermal district heating network. This study gives a better and deeper understanding of the effect of each individual design variable and its failure on the system behavior. In the future, with the increasing popularity of the solar community concept, finding the best combinations and tackling certain issues are important. Therefore, this information is useful for designers and engineers who are making preliminary decisions to design and build such systems.

5.4. Economic consequences

In a broader perspective, the energy system performance can have a great influence on the economy of the plant. The economic consequences can be divided into two major parts: (a) Hardware replacements: additional investment for maintenance or replacement of hardware, and (b) Software maintenance: no high investments needed as it only require changes in the algorithms or set points and are therefore very low cost. Both are defined in the following subsections.

5.4.1. Additional investment: replacement of the hardware

Some of the deviations caused by the change in the solar thermal collector efficiency, heat exchanger efficiency, tank stratification, space heating network temperature difference, BTES boundary layer thermal conductivity (high investments), and heat pump performance can be improved by replacing or maintaining these devices. However this would have an effect on the investments. Replacement can be very or moderately expensive. Therefore, the plant owners and contractors may have to bear the high cost of the equipment, and this would increase the overall investment in the system. A quantitative analysis of these investments needs further investigation and is out of the scope of this paper.

5.4.2. No additional investment: maintenance of the software and controls

Some of the deviations caused by a change in the warm tank, hot tank, space heating supply temperature set points, and solar collector circulation pump control can be improved by just changing the set point on the controller. This may not have any or at least a negligible impact on the investments, since only set points need to be adjusted in the controller device (unless there is a defect in the measurement instruments). As this kind of maintenance is not expensive compared with the hard investments, the plant owners and contractors may not have to bear the high cost. However, the end user may have to pay more for the increase in purchased electricity caused by such minor deviations or malfunctioning of the set points.

It is important to understand the importance of the design variables and its defects. This may result in underperformance of the overall energy system, and either the user or the investor must bear the high costs to compensate for the deviations in performance. It is also important to mention that some of these defects can be rectified with no additional costs, while some of the defects may need additional investments.

6. Conclusions

The novelty of this research was to identify and systematically investigate the influence of some generally known (real) technical failures on the performance of an optimized solar district heating system for a community. These technical issues are important to be considered during the construction of such system in order to provide the sensitivity to various failures. The energy system can be then constructed more smartly and prominently while considering such issues. It is generally found that every real plant failure and defect has a varied effect on performance and caused deviations in the estimated base case. Each scenario is created in order to include a failure that a system may face in real conditions. This is performed to show the amount of deviation expected in case of failure, defects, control failures, and malfunctions. The importance of such analysis is to provide insight of the system under adverse situations. This shows that to make solar heating system such technical failures need to be addressed to avoid underperformance of the system. Furthermore, this approach will lead to further popularization of in-depth analysis of failures of solar thermal system, especially in the era of renewable energy integration in the society. A brief summary of the key findings are:

- In ideal optimized base case, the purchased electricity varied from 49 kWh/m^2/yr to 25.9 kWh/m^2/yr, which correspond to the renewable fraction from 65 to 90%.
- The above stated ranges of the purchased electricity and renewable energy fraction of the optimized system are changed due to various malfunctions and issues in the components and controls.
- The most common issues that are found in the already existing solar thermal plants are, (1) heat exchanger efficiency, (2) solar thermal collector intercept efficiency, (3) tank stratification, (4) annual average heat pump coefficient of performance (COP), (5) space heating (SH) network temperature difference, (6) hot tank set points, (7) warm tank set points, (8) space heating (SH) supply temperature, (9) solar thermal circulation pump, and (10) thermal conductivity of boreholes boundary.
- It is observed that the following factors have a greater effect on the overall system performance: tank stratification, solar thermal circulation pump setting, heat pump COP, solar collectors intercept efficiency, BTES boundary layer thermal conductivity, space heating supply temperature set point and hot tank charging set point.
- The largest adverse impact is achieved by mixing the thermal stratification in the storage tanks to a uniform temperature. The increase in purchased electricity was 23–35%.
- The second largest adverse impact is achieved by change in the solar thermal circulation pump setting from variable to on/off control. The increase in purchased electricity was 1–22%.
- Third largest adverse impact is achieved by reduction in the heat pump COP. The increase in purchased electricity was 7–21%.
- Only the defect in the warm tank set point temperature slightly improved performance by 1–3%.
- Some of the defects caused in the heat exchangers, solar collectors, heat pumps, stratification of tank, BTES boundary layer thermal conductivity, and SPH return temperatures can be rectified with large investments that need to be borne by the investors and contractors.
- Some of the defects may not need large investments to be rectified, such as malfunctioning pump controls, tanks, and SH set points.

The study demonstrates the optimized solar thermal district heating system in Finnish conditions. The results can give useful information also for the solar district heating systems at lower latitudes. Various failures and defects in the technical parameters discussed in the paper show how important it is to consider all these non-idealities and issues in order to predict the deviations from the ideal scenario. Furthermore, it provided certain key

components that need to be considered during the implementation of such projects in a real environment. Poor estimations in defects, configuration, and design can lead to very poor performance. The results of this study may attract the interest of designers and contractors in using such ST systems.

Acknowledgements

This work has been funded by the Academy of Finland, grant number: 284977, under New Energy research program.

References

Alajmia, A., Wright, J., 2014. Selecting the most efficient genetic algorithm sets in solving unconstrained building optimization problem. Int. J. Sustain. Built Environ. 3 (1), 18–26.
ARANER, 2016. How Do Stratified Thermal Energy Storage Tanks Work? [Online] Available at: http://www.araner.com/blog/stratified-thermal-energy-storage-tanks/.
Attia, S., Hamdy, M., O'Brien, W., Carlucci, S., 2013. Assessing gaps and needs for integrating building performance optimization tools in net zero energy buildings design. Energy Build. 60, 110–124.
AXITEC Solar, 2016. AXI Power [Online] Available at: www.axitecsolar.com.
Bauer, D., Marx, R., Drück, H., 2016. Solar district heating systems for small districts with medium scale seasonal thermal energy stores. Energy Procedia 91, 537–545.
Bauer, D., et al., 2010. German central solar heating plants with seasonal heat storage. Sol. Energy 84 (4), 612–623.
BINE Information Service, 2000. Solar-assisted District Heating [Online] Available at: http://www.solites.de/download/literatur/bi_0800%20SUN_en.pdf.
Bose, B., 2016. Global warming: energy, environmental pollution and the impact of power electronics. IEEE Ind. Electron. Magzine 4 (1), 6–17.
Boyaghchi, F.A., Chavoshi, M., Sabeti, V., 2015. Optimization of a novel combined cooling, heating and power cycle driven by geothermal and solar energies using the water/CuO (copper oxide) nanofluid. Energy 91, 685–699.
Build it solar, 2006. Measuring Collector Performance and Efficiency [Online] Available at: http://www.builditsolar.com/References/Measurements/CollectorPerformance.htm#Efficiency.
CIT Energy Management AB, EU report, 2011. [Online] Available at: http://www.energy-management.se/;http://sunstore4.eu/download/member-area/wp5/EU%20report-WP5-deliverable%205%204_Feasibility%20simulation%20studies.pdf.
Dalenbäck, J.-O., 2005. Solar Heating – Swedish Experience [Online] Available at: http://www.energiasostenible.org/mm/file/19_4-SolarThermalSystemsSweden.pdf.
Dalenbäck, J.-O., Werner, S., 2012. Market for Solar District Heating, WP2 – European Market Study [Online] Available at: http://solar-district-heating.eu/portals/0/sdh-wp2-d2-3-market-aug2012.pdf.
Dalenbaeck, J.-O., 1998. European Large Scale Solar Heating Network [Online] Available at: http://ptp.irb.hr/upload/mape/kuca/08_Jan-Olof_Dalenback_EUROPEAN_LARGE-SCALE_SOLAR_HEATING_NETW.pdf.
Deb, K., Pratap, A., Agarwal, S., Meyarivan, T., 2002. A fast and elitist multiobjective genetic algorithm: NSGA-II. IEEE Trans. Evol. Comput. 6 (2), 182–197.
Dincer, I., Rosen, M., 2007. A unique borehole thermal storage system at university of Ontario institute of technology. Thermal Energy Storage Sustain. Energy Consum. 234, 221–228.
ESTIF - the European Solar Thermal Industry Federation, 2006. The Solar Keymark [Online] Available at: http://www.estif.org/solarkeymarknew/index.php.
European solar thermal industry federation(ESTIF), 2017 European solar thermal industry federation(ESTIF), 2017. Solar Thermal Markets in Europe [Online] Available at: www.estif.org.
Fakheri, A., 2006. Heat exchanger efficiency. J. Heat Tran. 129 (9), 1268–1276.
Faninger-Lund, H., 2003. Ekoviikin EU-aurinkolämpöjärjestelmien seurantajakso 2002 (SOLPROS) [Online] Available at: http://www.kolumbus.fi/solpros/reports/Ekoviikki_rap_2002.pdf.
Federal Ministry for the Environment, Nature Conservation and Nuclear Safety (BMU), 2013. Storing Solar Energy in the Ground [Online] Available at: http://www.bine.info/fileadmin/content/Presse/Projektinfos_2013/PM_01_2013/ProjektInfo_0113_engl_internetx.pdf.
Finnish Meteorological Institute, 2012. Weather and Climate in Finland [Online] Available at: http://en.ilmatieteenlaitos.fi/.
Fisch, M., Guigas, M., Dalenbäck, J., 1998. A review of large-scale solar heating systems in Europe. Sol. Energy 63 (6), 355–366.
Furbo, S., Mikkelsen, S., 1987. S Low-flow Operation an Advantage for Solar Heating Systems? Hamburg, s.n).
Gao, L., Zhao, J., Tang, Z., 2015. A review on borehole seasonal solar thermal energy storage. Energy Procedia 70, 209–218.
GREENoneTEC Solarindustrie GmbH, 2015. GK 3000 Series Large-surface Collectors [Online] Available at: http://www.greenonetec.com/fileadmin/user_upload/downloads/Produktdatenblaetter/3003_en_PDB_2015-09.pdf.
Haahtela, Y., Kiiras, J., 2013. Talonrakennuksen Kustannustieto 2013 (Building Construction Cost Data 2013) in Finnish. ISBN:9789525403213, Helsinki: Haahtela-kehitys.
Hahne, E., 2000. The ITW solar heating system: an oldtimer fully in action. Sol. Energy 69 (6), 469–493.
Hakala, P., et al., 2014. Evaluation of the Distributed Thermal Response Test (DTRT): Nupurinkartano as a Case Study [Online] Available at: http://tupa.gtk.fi/julkaisu/tutkimusraportti/tr_211.pdf.
Hakaste, H., Rinne, H., Jalo, T., 2008. Eko-Viikki-tavoitteiden ja tulosten erot energiankulutuksessa (Motiva Oy) [Online] Available at: http://www.motiva.fi/files/1576/Eko-Viikki_tavoitteiden_ja_tulosten_erot_energiankulutuksessa.pdf.
Hamdy, M., Hasan, A., Siren, K., 2011. Applying a multi-objective optimization approach for design of low-emission cost-effective dwellings. Build. Environ. 46 (1), 109–123.
Hamdy, M., Hasan, A., Siren, K., 2013. A multi-stage optimization method for cost-optimal and nearly-zero-energy building solutions in line with the EPBD-recast 2010. Energy Build. 56, 189–203.
Hannoschöck, N., 2016. Research Gate [Online] Available at: https://www.researchgate.net/post/What_is_the_average_efficiency_of_gas_water_heat_exchanger.
Heller, A., 2000. 15 years of R&D in central solar heating in Denmark. Sol. Energy 69 (6), 437–447.
Honkonen, M., 2016. Thermal ENergy Storage Concepts and Their Feasibility, Espoo. Master's thesis(Rak-32). Aalto University, Civil engineering, Rock mechanics, Finland.
International Energy Agency Solar Heating and Cooling Programme, IEA-SHC, Task 32, 2015. Task 32-Advanced Storage Concepts for Solar and Low Energy Buildings [Online] Available at: http://archive.iea-shc.org/task32/.
Internatonal Energy Agency-Task VII, 1990. Central Solar Heating Plants with Seasonal Storage- Status Report. Swedish Council for Building Research, Chalmers.
Jylhä, K., et al., 2015. Hourly test reference weather data in the changing climate of Finland for building energy simulations. Data in Brief 4, 162–169.
Koppen, C.V., Thomas, J., Veltkamp, W., 1979. The Actual Benefits of Thermally Stratified Storage in a Small and Medium Size Solar Systems. Atlanta, s.n).
Lundh, M., Dalenbäck, J.-O., 2008. Swedish solar heated residential area with seasonal storage in rock: initial evaluation. Renew. Energy 33 (4), 703–711.
Mangold, D., 2007. Seasonal storage – a German success story. Sun Wind Energy 1, 48–58.
Mangold, D., Schmidt, T., 2003. The Next Generations of Seasonal Thermal Energy Storage in Germany. Solites-Steinbeis Research Institute for Solar and Sustainable Thermal Energy Systems, Stuttgart, Germany.
Mauthner, F., Herkel, S., 2016. SHC Task 52, Technology and Demonstrators: Technical Report Subtask C- Part C1:Classification and Benchmarking of Solar Thermal Systems in Urban Environments [Online] Available at: http://www.solarthermalworld.org/sites/gstec/files/news/file/2016-05-28/iea-shc_task_52_stc1-classification_and_benchmarking_2016-03-31_report.pdf.
McDowell, T.P., Thornton, J.W., 2008. Simulation and Model Calibration of a Large-scale Solar Seasonal Storage System. Berkeley, California s.n).
Meliß, M., Späte, F., 2000. The solar heating system with seasonal storage at the solar-campus Jülich. Sol. Energy 69 (6), 525–533.
Ministry of the Environment, Department of the Built Environment, 2010. D5 National Building Code of Finland, Calculation of Power and Energy Needs for Heating of Buildings, Guidelines 2012,DRAFT 28 September 2010 [Online] Available at: http://www.puntofocal.gov.ar/notific_otros_miembros/fin43_t.pdf.
Montagud, C., Corberán, J.M., Ruiz-Calvo, F., 2013. Experimental and modeling analysis of a ground source heat pump system. Appl. Energy 109, 328–336.
Neves, D., Silva, C.A., 2014. Modeling the impact of integrating solar thermal systems and heat pumps for domestic hot water in electric systems – the case study of Corvo Island. Renew. Energy 72, 113–124.
NIBE, 2017. Technical Data [Online] Available at: http://www.nibe.eu/nibedocuments/16111/F1345-60.pdf.
Nielsen, J.E., 2012. IEA-SHC task 45: large solar heating/cooling systems, seasonal storage, heat pumps. Energy Procedia 30, 849–855.
Nussbicker-Lux, J., 2012. The BTES project in Crailsheim Germany-monitoring results. In: Lleida,Spain, 12th International Conference on Energy Storage-innostock.
Ochs, F., et al., 2008. Solar Assisted District Heating System with Seasonal Thermal Energy Storage in Eggenstein [Online] Available at: http://www.itw.uni-stuttgart.de/dokumente/Publikationen/publikationen_08-10.pdf.
Official Statistics of Finland (OSF), 2016. Energy Supply and Consumption [e-publication] [Online] Available at: http://www.stat.fi/til/ehk/index_en.html.
Palonen, M., Hamdy, M., Hasan, A., 2013. MOBO a New Software for Multi Objective Building Performance Optimization. Chambery, France s.n).
Palonen, M., Hasan, A., 2017. MOBO Beta 0.3b Manual Version 1.4 [Online] Available at: https://www.researchgate.net/publication/273307166.
Raab, S., Mangold, D., Müller-Steinhagen, H., 2005. Validation of a computer model for solar assisted district heating systems with seasonal hot water heat store. Sol. Energy 79 (5), 531–543.
Rad, F.M., Fung, A.S., Leong, W.H., 2013. Feasibility of combined solar thermal and ground source heat pump systems in cold climate, Canada. Energy Build. 61, 224–232.
Rehman, H. u., Hirvonen, J., Sirén, K., 2016. Design of a simple control strategy for a community-size solar heating system with a seasonal storage. Energy Procedia 91, 486–495.
Rehman, H. u., Hirvonen, J., Sirén, K., 2017. A long-term performance analysis of three different configurations for community-sized solar heating systems in high latitudes. Renew. Energy 113, 479–493.

Riku Pasonen, K.M.R.A., 2012. Arctic Solar Energy Solutions, VTT Technical Research Centre of Finland, ISBN 978-951-38-7825-2 [Online] Available at: http://www.vtt.fi/inf/pdf/technology/2012/T15.pdf.

Schmidt, T., Mangold, D., Muller-Steinhagen, H., 2004. Central solar heating plants with seasonal storage in Germany. Sol. Energy 76 (1–3), 165–174.

Sibbitt, B., et al., 2015. Groundbreaking Solar [Online] Available at: http://www.hpbmagazine.org/attachments/article/12213/15Su-Drake-Landing-Solar-Community-Alberta-Canada.pdf.

Sibbitt, B., et al., 2011. Measured and simulated performance of a high solar fraction district heating system with seasonal storage. In: Kassel, Proceedings of the ISES Solar World Congress.

Sibbitt, B., et al., 2012. The performance of a high solar fraction seasonal storage district heating system – five years of operation. In: Energy Procedia, 1st International Conference on Solar Heating and Coolingfor Buildings and Industry (SHC 2012), vol. 30, pp. 856–865.

Solar district heating, 2012. Solar District Heating Guidelines-storage [Online] Available at: http://solar-district-heating.eu/Portals/0/Factsheets/SDH-WP3_FS-7-2_Storage_version3.pdf.

Solar Energy Laboratory, University of Wisconsin-Madison, 2012. TRNSYS—a Transient Systems Simulation Program, Version 17.1. Solar Energy Laboratory, University of Wisconsin-Madison, 2009–2012. [Online] Available at: http://sel.me.wisc.edu/trnsys.

SOLPROS, 2004. Ekoviikin EU-aurinkolämpöjärjestelmien jatkoseuranta-LOPPURAPORTTI [Online] Available at: http://www.kolumbus.fi/solpros/reports/Ekoviikki_loppuraportti_2004.pdf.

Struckmann, F., 2008. Analysis of a Flat-plate Solar Collector [Online] Available at: http://www.ht.energy.lth.se/fileadmin/ht/Kurser/MVK160/Project_08/Fabio.pdf.

The European Parliament and the Council of the European Union, 2010. Directive 2010/31/EU of the European Parliament and of the council of 19 May 2010 on the energy performance of buildings. EU Inst. Official J. Eur. Union 53, 13–35. ISSN 1725-2555, L 153.

Tordrup, K., Poulsen, S., Bjørn, H., 2017. An improved method for upscaling borehole thermal energy storage using inverse finite element modelling. Renew. Energy 105, 13–21.

Truong, N.L., Gustavsson, L., 2014. Solar heating systems in renewable-based district heating. Energy Procedia 61, 1460–1463.

Urbaneck, T., et al., 2015. Solar district heating in East Germany – transformation in a cogeneration dominated city. Energy Procedia 70, 587–594.

Weissmann, C., Hong, T., Graubner, C.-A., 2017. Analysis of heating load diversity in German residential districts and implications for the application in district heating systems. Energy Build. me 139, 302–313.

World Geodetic System WGS84 standard, 2012-2016. [Online] Available at: http://www.latlong.net/place/helsinki-finland-1668.html.